UDC 621. 224. 2-155 : 621. 313. 322

ELECTRICAL EQUIPMENT FOR NISHIKADOHARA NO. 3 POWER STATION HOKURIKU ELECTRIC POWER CO., INC.

Takashi Konota
Electric Power Engineering Dept.
Tsuneo Ueda
Mitsuru Takahashi
Kawasaki Factory

I. INTRODUCTION

The 50,000 kw vertical-shaft Deriaz type water turbine, 53,000 kva vertical-shaft synchronous generator, 53,000 kva 3-phase transformer and the other switching equipment supplied to the Nishikadohara No. 3 power station of the Hokuriku Electric Power Co., Inc. successfully passed all official tests and began operation in May, 1968.

Original plans for this power station called for a Francis turbine. However, it was anticipated that a considerably long period of partial load operation would be required to meet of water discharge requirments for downstream irrigigation. For this reason, investigations were conducted under all anticipated operating conditions comparing the economy and performance of one Francis water turbine, two Francis water turbines, and one Deriaz type water turbine. Results of these investigations showed that the Deriaz type water turbine was the most economical.

II. DERIAZ TYRE WATER TURBINE

1. Turbine Specifications

Type: Vertical shaft movable-blade Deriaz type water turbine

Effective head (m):	99	97	92.5
Discharge (m^3/sec):	56	57.6	56
Turbine output (kw):	50,000	50,000	46,500
Rated speed (rpm):	257		
Specific speed (m-kw):	189		
Runaway speed (rpm):	520		

2. Performance of Turbine

1) Model tests

Since this turbine was to be one of the largest high head Deriaz type turbines in the world, the following tests were carried out prior to manufacture of the prototype turbine; efficiency tests, cavitation tests, and runaway speed tests for runners with different diagonal flow angles. From these tests, the most suitable runner was chosen and measurements were taken for all the characteristics required for designing and manufacturing of the prototype turbine,

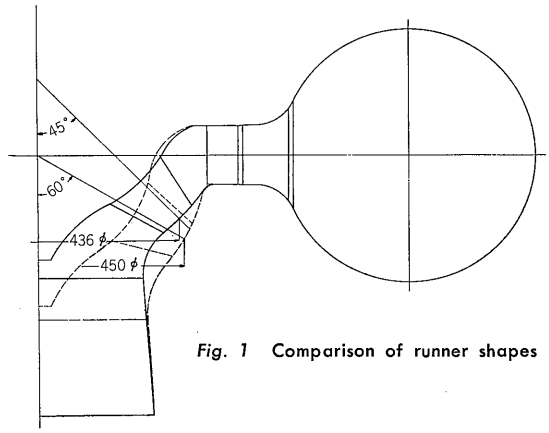

Fig. 1 Comparison of runner shapes

such as hydraulic thrust, required operating moment of runner blade, water pressure fluctuation etc. These tests and measurements will be outlined below.

(1) Diagonal flow angle tests

The most important factor in determining the characteristics of the Deriaz type tubine is the runner vane diagonal flow angle (the conic angle formed by the runner blade stems).

Generally speaking the most suitable diagonal flow angle increases from 90° and 140° in accordance with increases in the specific speed.

A comparison of runner blade shapes with different diagonal flow angles of the same specific speed is shown in *Fig. 1*. Generally, when the diagonal flow angle is large, the ratio of the diameters of the runner vane inlet and outlet on the boss side is small; therefore there is a large bend of the stream line along the boss side. Also, since the difference in the diameters of the runner vane tip end and boss end is large, the blade twist tends to increase.

A diagonal flow angle of 90° is generally used in Deriaz type turbines when the head is around 100 m. However, Fuji Electric assumed from the results of previous model tests that an angle of 120° would be the most appropriate and two model runners, one with an angle of 90° and one with 120° as shown in *Fig. 2* were tested. A detailed comparison of their characteristics gives the following results.

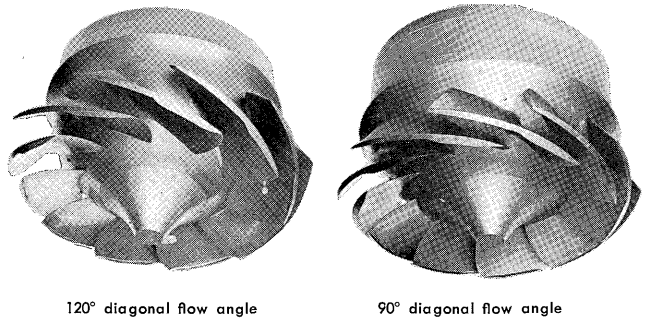

120° diagonal flow angle　　90° diagonal flow angle

Fig. 2 Model turbine runners

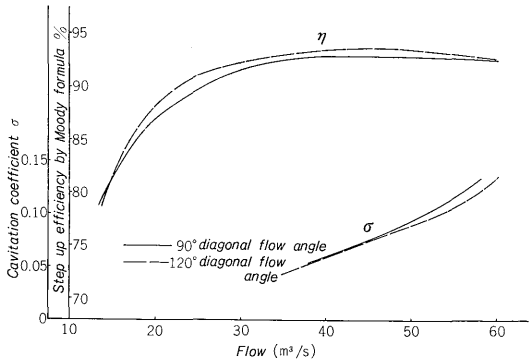

Fig. 3 Model test results

(a) The weighted mean efficiency of the 120° runner is about 0.6% higher than that of the 90° runner (See *Fig. 3*).

(b) The critical cavitation coefficient of the 120° runner is about 0.01 less than in the 90° runner (See *Fig. 3*).

(c) The runaway speed of the 120° runner is about 15% lower than in the 90° runner.

Therefore, the 120° runner is superior in all of the above characteristics and for this reason it was finally decided to adopt the 120° runner for the prototype turbine.

(2) Vibration tests

In all of the Deriaz type turbines and Deriaz type pump-turbines previously put into operation in Japan, it was often reported that considerable water pressure fluctuations occurred during load rejection, and vibration and noise occured when the turbine was operated at a load of less than 25%.

These phenomena were also confirmed in the previous model tests and *Fig. 4* shows measurements of pressure fluctuations at the casing inlet of a Deriaz type pump turbine with a diagonal flow angle of 98°. When the runner blade angle was large; the rotating speed increased, the discharge in the vicinity of the runaway speed decreased and the water pressure fluctuation amplitude suddenly became very large. However, when the runner blade angle was small, the reduction of the discharge and increase of the pressure fluctuation amplitude in the region near the runaway speed were not so pronounced.

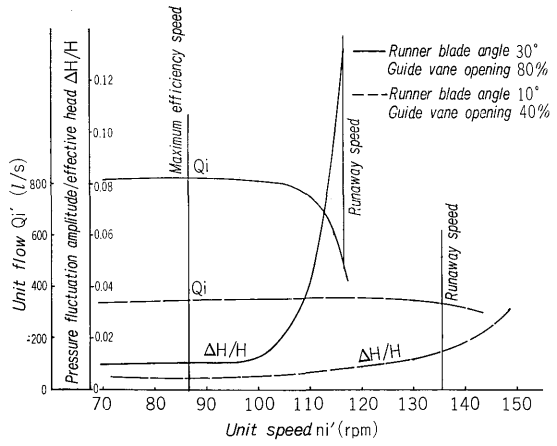

Fig. 4 Casing inlet pressure fluctuations

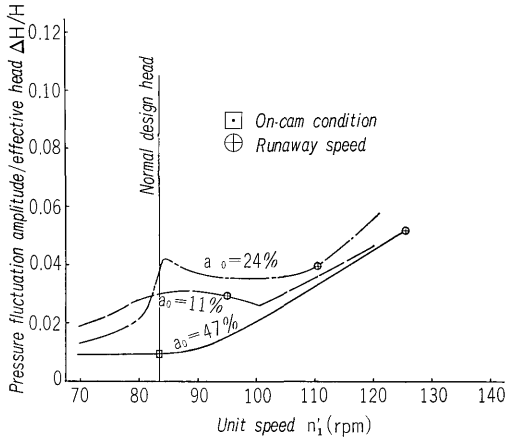

(a) Runner blade angle: 9.5°

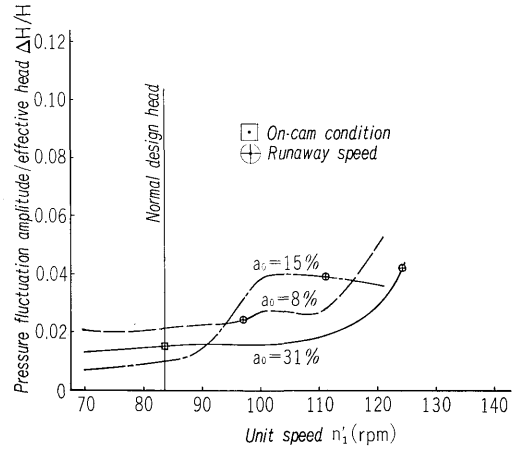

(b) Runner blade angle: 5°

Fig. 5 Casing inlet pressure fluctuations

Since the above mentioned pressure fluctuations were also anticipated in the Nishikadohara No. 3 power station turbine, the relation between the pressure fluctuations and rotating speed was investigated by changing the runner blade angle and the guide vane opening in a model turbine. An example of the results of these investigations is shown in *Fig. 5*.

If the appropriate relation between the runner blade closing time and guide vane closing time is chosen on the basis of these results, it is anticipated that the pressure fluctuation amplitude in the prototype turbine during load rejection could be kept to 6 m or below.

To insure optimum cavitation characteristics in a high head Deriaz type turbine, the runner blade pitch cord ratio must be small and the vane overlapping large. In this case minimum runner blade angle becomes large and the on-cam output at the minimum runner blade angle is approximately 20% of the maximum output. Thus for outputs below this value, vibration and noise tend to increase considerably due to rotating flow in the draft.

According to results using model turbines, the pressure fluctuation at the casing inlet of the prototype turbine during no-load operation should be about 2.5 m and therefore the equipment was designed in such a way that it is possible to attach forced air equipment using a jet pump for partial load operation below the minimum on-cam load.

2) Turbine tests at site

At the end of April, test operation was begun and the official tests were completed on the 18th and 19th of May. Operation is now highly satisfactory.

(1) Efficiency tests

Effficiency tests were carried out by the current meter method and the ultrasonic method.

The results of the efficiency tests are shown in *Fig. 6*. The current meter method showed a very high maximum efficiency of 93.4%, which was almost the same as the step up efficiency by the Moody formula. With the ultrasonic method, the maximum efficiency was also 93.4% and was almost the same as the efficiency measured by the current meter method in the vicinity of the maximum output. However, at partial loads, the ultrasonic method efficiency was about 2% lower than the current meter efficiency.

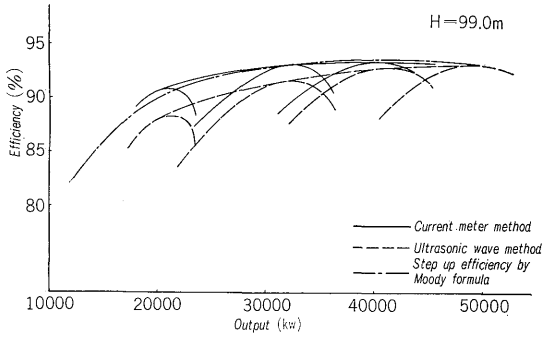

Fig. 6 Site efficiency test results

(2) Load rejection tests

As was anticipated from the model turbine, pressure fluctuations occurred which were superimposed on the pressure variation caused by the water hammering. However, it was confirmed that the momentary pressure and speed rise were both within the guaranteed values.

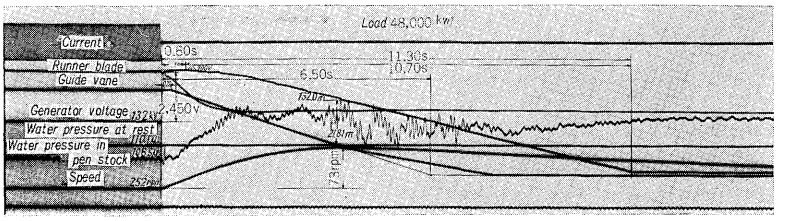

Fig. 7 Record of full-load rejection test

A record of a load rejection test is shown in *Fig. 7*.

(3) Vibration measurements

Vibrations at the bearing pedestal during normal load operation were usually very low, less than 2 μ. However, noise developed due to rotating flow in the draft tube in the vicinity of no-load conditions (vibration was only 6～25 μ). In order to improve this condition, forced air equipment using a jet pump was installed which automatically supplies air at the guide vane opening of 5～25%. Results had shown that quiet operation was possible over the full load range.

3. Turbine Construction

The machine arrangements are shown in *Figs. 8～10*. *Fig. 11* shows a cross-sectional view of the water turbine and generator, while *Fig. 12* shows the turbine as assembled in the shop.

1) Spiral casing and speed ring

Since the casing is large with an inlet diameter of 3200 mm, the speed ring was divided into 5 sections and the casing into 7 parts which were welded together at the site. From the investigation comparing 60 kg/mm^2 class high tension steel plates and rolled steel for welded structure SM50, it was found that the high tension steel plates were more economical and these were therefore used for the casing.

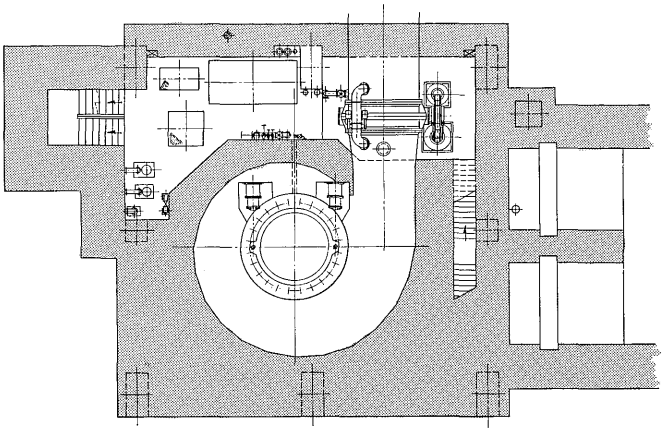

Fig. 8 Machine arrangement (Sump tank floor)

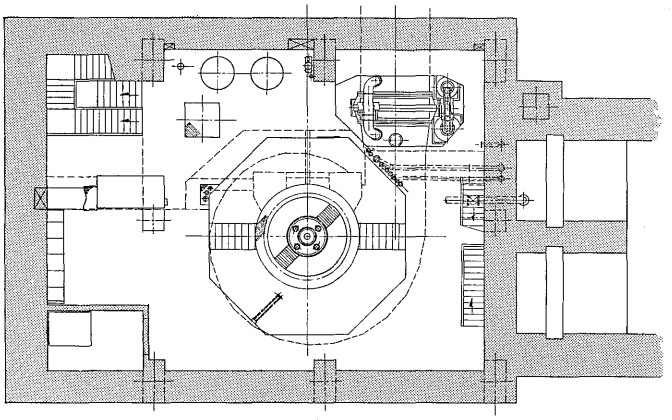

Fig. 9 Machine arrangement (Turbine floor)

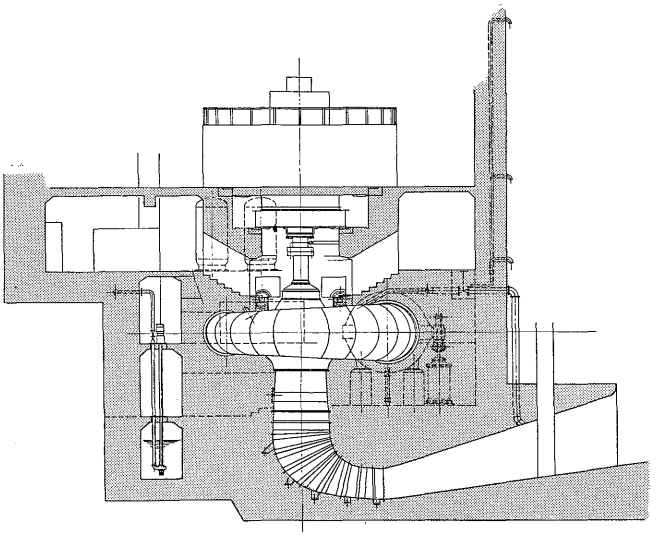

Fig. 10 Machine arrangement (Sectional view)

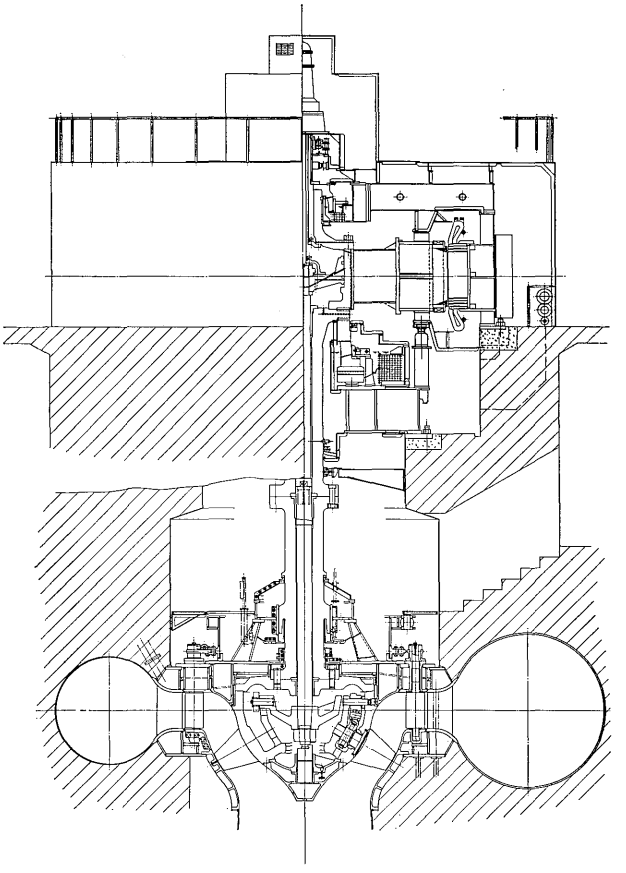

Fig. 11 Sectional view of water turbine and generator

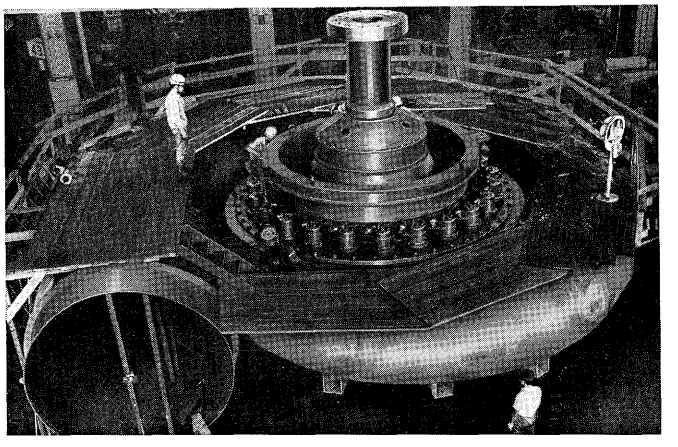

Fig. 12 Turbine as assembled in shop

After the site welding was completed, pressure tests were conducted and it was confirmed that there were no leaks or other abnormalities. During the pressure tests, the stress and displacement of all casing parts was measured and a check was made to find out if any of the values were abnormal. From these results it was confirmed that all the design values were met.

The pressure embedding method with half of the maximum static head was adopted for concreting the spiral casing. With this method, local surface presure on concrete parts due to displacement of the casing during operation and the stress on the concrete barrel are both minimized.

2) Head cover and bottom ring and discharge ring

The head cover consists of two parts: the inner head cover and outer head cover; so that the runner can be removed without disassembling the guide vane. The outer top cover is made of welded steel sheets and the surface which faces the guide vane is lined with 13Cr stainless steel sheets. In Deriaz type water turbines, the runner is very heavy and the distance between the center of gravity of the runner and the main bearing is long so that it is easy for vibrations to occur. Hence the distance between the center of gravity of the runner and the main bearing was shortened, and the bearing support was constructed of sufficienty rigid material. The bearing cover is so designed that it supports the weight of the runner and turbine shaft when the turbine shaft and generator shaft are disconnected. The bottom ring is made of cast iron with a 13Cr stainless steel lining facing the guide vanes. The discharge ring is made of stainless cast steel and machining was performed with great care using a vertical mill with automatic profiling gear.

3) Guide vane regulating mechanism

The guide vane is made of one steel casting. The upper and lower surfaces are covered with 18–8 stainless steel plates. The guide vane arm consists of two parts and a breaking pin is provided which is provided with a turnbuckle to adjust the position of individual guide vanes.

Inside the turbine pit two servomotors are placed. Mechanical locking equipment is located between the head cover and the regulating ring.

4) Runner

The runner blade has a diagonal flow angle of 120° and consists of 10 blades with a nominal diameter of 3200 mm. The runner boss is made of 13Cr cast steel and runner blades which are used under especially rigorous conditions are made of materials with special properties. In order to prevent cavitation erosion of the outer rim of the runner blade due to gap cavitation, an erosion proof piece is attached. An improved system which Fuji Electric has already used in other Deriaz pump turbines is adopted as the runner blade operating mechanism.

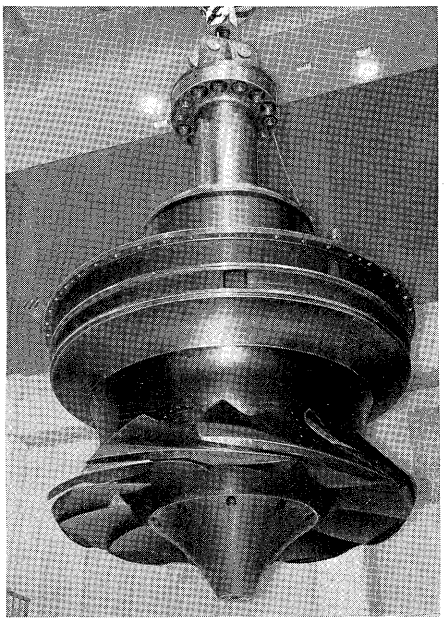

Fig. 13 Runner and inner top cover

5) Runner servomotor

The runner servomotor is of the vertical motion type used in the Kaplan water turbine and is installed in the center of the generator rotor. This movement is transferred via the operation rod in the turbine shaft hole to the runner operating disk. The oil supplying equipment to the runner servomotor is located in the upper part of the generator.

6) Main shaft and shaft bearing

The water turbine shaft is made of forged steel having a diameter of 710 mm. The shaft seal consists of two carbon rings which surround the main shaft and are held firmly in place with springs. The main shaft bearing has a special groove which makes use of oil viscosity and pump action. A water jacket system is used in which the cooling water is circulated in a jacket of the main bearing.

4. Inlet Valve

The inlet valve is a butterfly valve with an inner diameter of 3200 mm. Since this power station is tele-controlled from another power station, the following safety methods to stop the turbine when the oil pressure drops below allowable value, were investigated.

(1) Automatic guide vane closing by hydraulic closing moment
(2) Guide vane closing by means of a water operated servomotor
(3) Inlet valve closing by means of a water operated servomotor
(4) Inlet valve closing by means of a weight

Automatic closing of the guide vane to the no-load opening is possible in movable-vane turbines under on-cam conditions. However, when this on-cam condition is broken and the runner vane opening is less than at the on-cam conditions, automatic closing becomes impossible. Since automatic closing is so unreliable, only points (2), (3) and (4) remain. Point (2) presents considerable difficulty in relation to maintenance and point (4) is inferior to point (3) concerning weight and space requirements. Therefore point (3) was adopted in the light of reliability and economy. Under normal conditions, an oil servomotor is used for valve opening and closing but when the oil pressure is low or overspeed conditions are reached, the inlet valve is closed by means of a water operated servomotor through a special lever.

5. Governor and Pressure Oil Equipment

Fuji Electric's standard cabinet-type electro-hydraulic governor was adopted. All operations can be performed from the front of the panel. The limit switch is of the contactless type. In order to improve the safety of control the main electromagnetic valves: $21S_1$, 65S and 97S, have duplicate trip coils which are operated by a separate electric source even if dc battery source fails. This means a considerable improvement in the safety of the valves. The pressure oil system has two vertical shaft motor driven screw pumps with a capacity of 600 *l*/min at 25 kg/cm^2. The pressure oil tank has a capacity of 10,300 *l* and because of the space limitation of the powerhouse, two inter-connected tanks are used.

III. GENERATOR

1. Generator Specifications

Rated output : 53,000 kva
Rated voltage : 13,200 v

Rated frequency: 60 Hz
Power factor: 90.5% (lagging)
Rated speed: 257 rpm
Excitation system: OH-type static excitation system

2. Outline

As shown in *Fig. 11*, the generator is a semi-umbrella type. Guide bearings are arranged in the upper and low parts of the generator rotor respectively. The thrust bearing is located inside the oil tank on the lower bracket together with the lower guide bearing. The center of the rotor contains the runner blade servomotors, and the oil supply equipment for operation of the runner blade is arranged in the uppermost part of the generator.

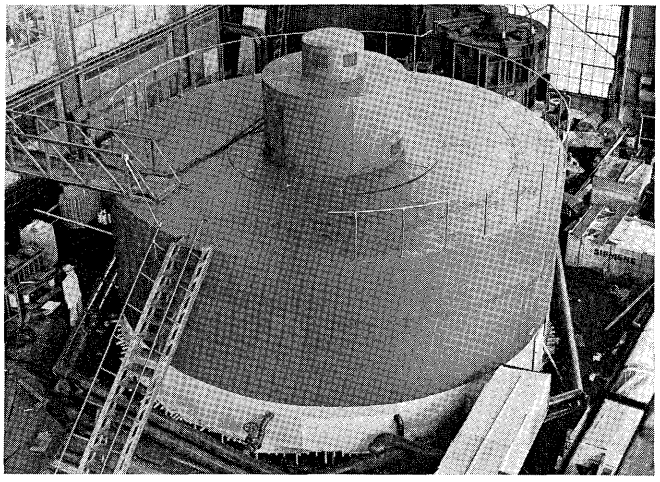

Fig. 14 Generator as assembled in shop

3. Problems which Arise During the Basic Planning Stages

When designing of this equipment, selection of the rated voltage presented a problem. Invesgation was made to select the best rated voltage on not only for the generator itself but also for the circuit breaker, disconnecting switch, potential transformer, and isolated phase bus, etc. The results showed that 13.2 kv was more economical and it was decided to use this value.

The 13.2 kv stator winding was made more effective by the use of special "Roebel" transposition and connection methods. The following is given for reference:

$$C=\text{kva}/Di^2 \cdot L \cdot n \quad \cdots\cdots(1)$$

where Di: Stator inner diameter
L: Length of iron core
n: Rated speed

In recent water turbine generators, output coefficient C calculated from equation (1) is more the 20~30% larger than that of previously designed ones. Thus the equipment is small and therefore more economical. Even the GD^2 required from the water turbine side becomes rather small since larger momentary speed variation occurs, but it is still rather large, when compared with the natural generator GD^2.

$$GD^2=kDi^4 \cdot L \quad \cdots\cdots(2)$$

where k: constant

From equation (1), (2), the following equation is obtained.

$$GD^2=k\left(\frac{\text{kva}}{n}\right)\frac{Di^2}{C} \quad \cdots\cdots(3)$$

When kva and n decided, Di^2/C must also be constant to keep the required GD^2 constant. Therefore if C is large, then Di must be large. Due to recent advances in design and materials, the value of k has become small so that Di must be even larger.

Therefore, there is a strong tendency for the inner diameter Di to be very large and the length of the iron core L to be short when compared with previous equipment of the same GD^2.

When a one-turn coil is used as the stator winding in large capacity generators, there are many advantages, and the smaller number of slots, the better from the standpoint of economy.

In case the number of slots is small, the slot pitch becomes large and the slot width can be increased so that each conductor used in "Roebel" transposition is naturally wider.

Fig. 15 shows bars which employ the "Roebel" transposition. When a current I flows in these bars, the current density i is as shown in equation (4).

$$i=\frac{I}{b \cdot d \cdot 2m} \quad \cdots\cdots(4)$$

where b: Width of wire
d: Thickness of wire
m: Number of longitudinal levels of wire

When i is assumed from the temperature rise etc. and b is determined, then the product $d \cdot m$ can be determined. The value of m is decided by the capability of manufacturing the "Roebel" transposition bars. In other words, when the value of the conductor braid pitch $\lambda=L/2m$ is not above a certain value, there is a danger of layer shorts between the conductors and troubles will arise during manufacturing so that it becomes impossible to braid the wires. As was described previously, m can not be too large in machines where Di is large and L is small, so that d becomes large.

However, when the conductor thickness d is rather large, eddy current flows because of the voltage

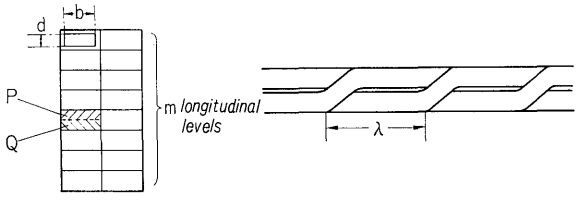

Fig. 15 Roebel transposition

difference between the top and bottom of the conductor interior and for this reason, the loss increases. When viewed from the exterior, the ac resistance and the loss increases and therefore no matter how carefully the " Roebel " transposition is carried out, it is not effective.

In this machine a skilful method is used to solve this problem. The conductor thickness d is maintained within a permissible value and a value m' is used which is up to twice the value of m which is limited to $\lambda = L/2m$. However, 2 longitudinal conductors make one group and the " Roebel " transposition is applied by considering these two conductors as a single one. In this way, it becomes equivalent to a " Roebel " transposition of $m = m'/2$. This can be called a " 2 level Roebel " transposition.

When this method is used it is necessary to consider the end connection between coils. In the previous method where all conductors are gathered in one part or in the method where connection is made by dividing into several blocks, a voltage difference develops between the two levels of conductor (between P and Q as shown in *Fig. 15*) which causes a current to circulate, making the division ineffective. To prevent this, one end is connected as previously and (as shown in *Fig. 16*) in the other end the upper conductor P of the upper bar and the lower conductor Q of the lower bar as well as the lower Q of the upper bar and the upper P of the lower bar are independently connected each other.

With this method, the voltage which develops in each conductor forms a closed circuit as shown by the arrows and the overall voltage value becomes very small. The resistance of the closed circuits is large so that the circulating current in the circuit is very small. Therefore the stray-load loss also becomes very small.

The actual values of stray-load loss measured in factory tests agreed well with the calculated values which confirmed the above-mentioned calculations.

4. Construction Features

1) Direct coupling with the Deriaz type turbine

On the Deriaz type turbine, the gap between the runner blade and the discharge ring is selected as small as possible to minimize the gap cavitation and lowering of the efficiency. However, no contact between the runner and the discharge ring must occur even under the worst conditions. Therefore,

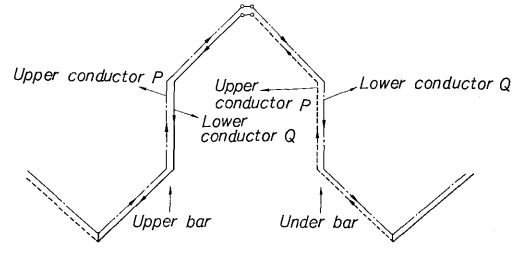

Fig. 16 Special connection method

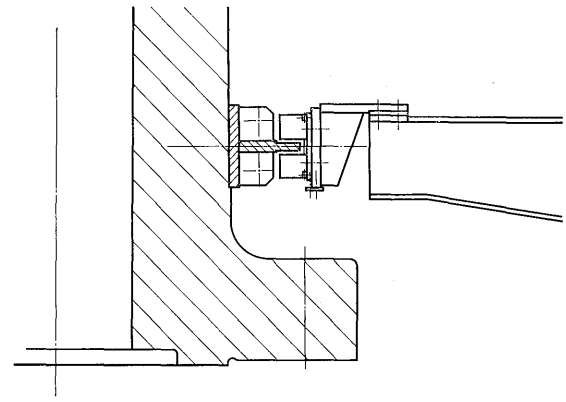

Fig. 17 Attachment of shaft displacement detector

it is necessary to provide equipment which detects any displacement of the runner gap during operation. Upward or downward displacement of the runner can be caused by expansion or contraction of the shaft due to water thrust or temperature variations in the construction materials. In this type turbine, the surface of the discharge ring is inclined so that mere upward or downward displacements of the shaft result in shifts of the runner gap. Therefore a circular plate was installed on the shaft and one differential reactor each is located on the top and bottom of this plate. Runner blade displacements can be supervised by detection equipment which measures the shaft displacement by means of variations in this reactance. When the runner is displaced downward below a certain limit, the equipment is immediately stopped or an alarm sounds. The shaft displacement detector is shown in *Fig. 17*. The gap was designed so as to fulfill the following conditions.

(1) The specified gap can be maintained during rated operation.

(2) Naturally, no gap contact must occur even under unusually high water thrusts, or when the babbitt metal of the thrust bearing has melted away because of such thrusts.

For this reason, the lower bracket which supports the thrust bearing must be sufficiently rigid. The amount of deflection of the lower bracket and of the thrust spring was tested at the factory under actual loads and these values were shown to be the same as the design values.

2) Dismantling and checking of the thrust bearing

The thrust bearing must be such that it can be checked or replaced with a spare without removing the generator rotor.

Fig. 18 illustrates the method of removing the thrust bearing. The rotating part is pushed slightly upwards by means of the oil jack and the guide bearing and bearing support are lifted out.

When the bearing oil tank is pushed upwards with the special oil jack, the thrust bearing is exposed to view and it can be easily lifted out for checking or replacement. When this method is employed,

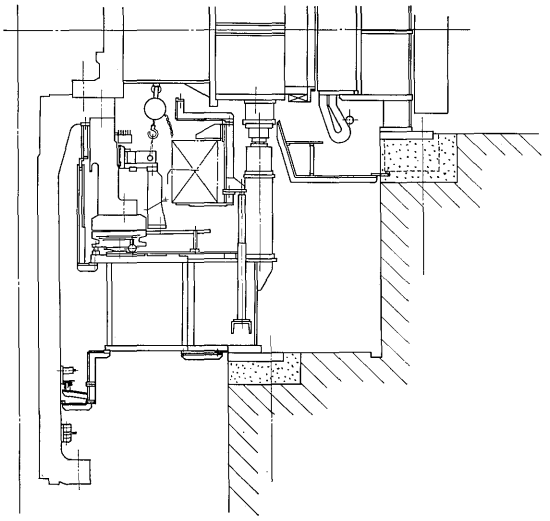

Fig. 18 Method of removing thrust bearing

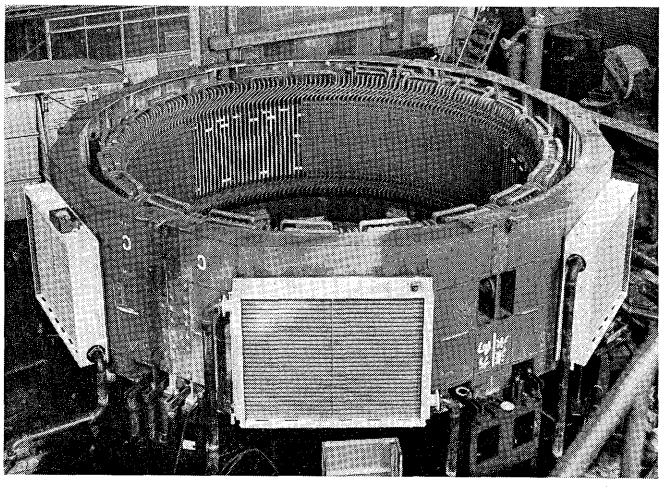

Fig. 19 Stator

the time required for checking the thrust bearing can be reduced considerably.

3) Stator

The stator core is made of laminated high grade silicon steel sheets.

A new "Laschen" construction which has many advantages is used to secure the core to the stator frame. The stator frame is of the "box" type construction and is divided into 3 parts for transport. The laminated core is tightened after thermally drying to prevent core aging phenomena during operation. It was confirmed that no abnormal vibrations occur due to reasonance caused by the power source frequency at double the frequency. The winding consists of a one-turn coil with F-resin (main constituent: epoxy type resins) insulation which exhibits excellent corona and thermal resistance characteristics.

4) Rotor

The magnetic pole core is made of laminated high tensile strength steel plates which are riveted together through special steel end plates. The pole core is attached on the yoke by the dove tail method and

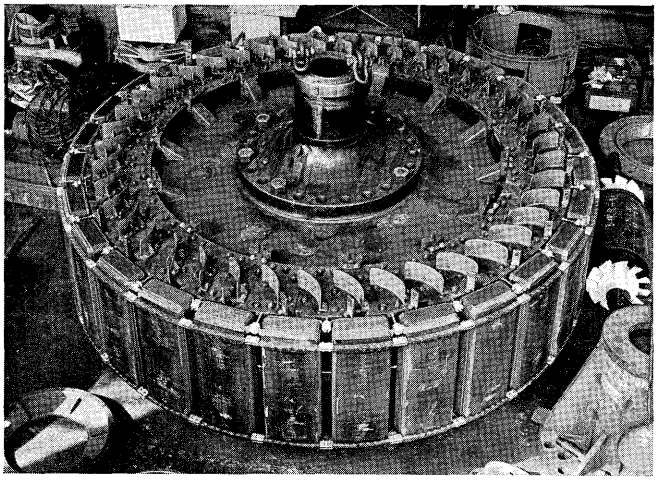

Fig. 20 Rotor

held in place by tapered keys. The winding is attached to the core by means of thermal compression at suitable temperatures and pressures in such a way that it is sufficiently adaptable to variations in the insulation as well as thermal expansion and centrifugal force.

Since the yoke must be divided during transport, it is made of laminated sector-type high tensile strength thin steel plates held together in a single ring shape by means of reamer studs. The yoke is shrink-fitted onto the center of the rotor.

The rotor center is of the disc type which reduces the windage loss and is also stronger than the previously used spider-type. The center boss also serves as the runner blade servomotor cylinder.

5. Test Results

The results of the test conducted at the factory and on the site are given below.

1) Short-circuit ratio

Since this is a self-excited compound ac generator, the excitation response is rapid and therefore the ability to contribute to the system stability is higher than in directly coupled exciter systems. For this reason, the short-circuit ratio is guaranteed to be over 0.9 which is favorable from both the mechanical and economic points of view.

2) Efficiency tests

Measured efficiency at the factory test achieved the guaranteed value without the tolerances which are granted in the contract.

3) Temperature rise test

A no-load rated voltage temperature rise test and a copper loss temperature rise test were carried out on the stator winding at the factory and the summation of these values were assumed to be equivalent to actual load conditions. On-site test results using an embedded temperature detector indicated almost the same value as the factory tests.

4) Voltage rise during load rejection

The guaranteed voltage rise is 30% in respect to a guaranteed momentary turbine speed rise of 40%

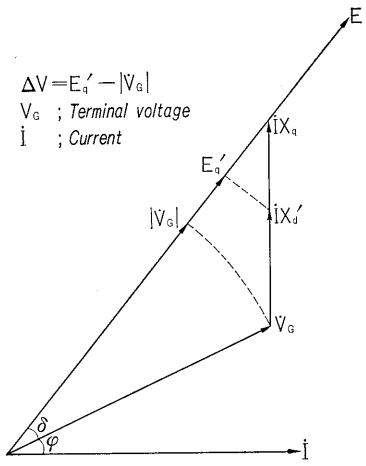

Fig. 21 **Determination of voltage rise by vectorical method**

under a full load rejection. In most self excited compound systems, the current transformer is out of action at the instant load rejection takes place so that the exciting current is also rapidly reduced. In addition to above, this excitation system is provided with "Transidyn" control equipment—all transistorized equipment —so that secondary control is very rapid. The maximum voltage rise determined vectorially as shown in *Fig. 21* is reached at the instant of load rejection and the voltage rapidly falls away to the set value.

This was clearly shown in the results of full-load rejection tests at the site as is indicated in the record in *Fig. 7*. The voltage rise of 18.56% at the full load rejection is well within the guaranteed value of 30%.

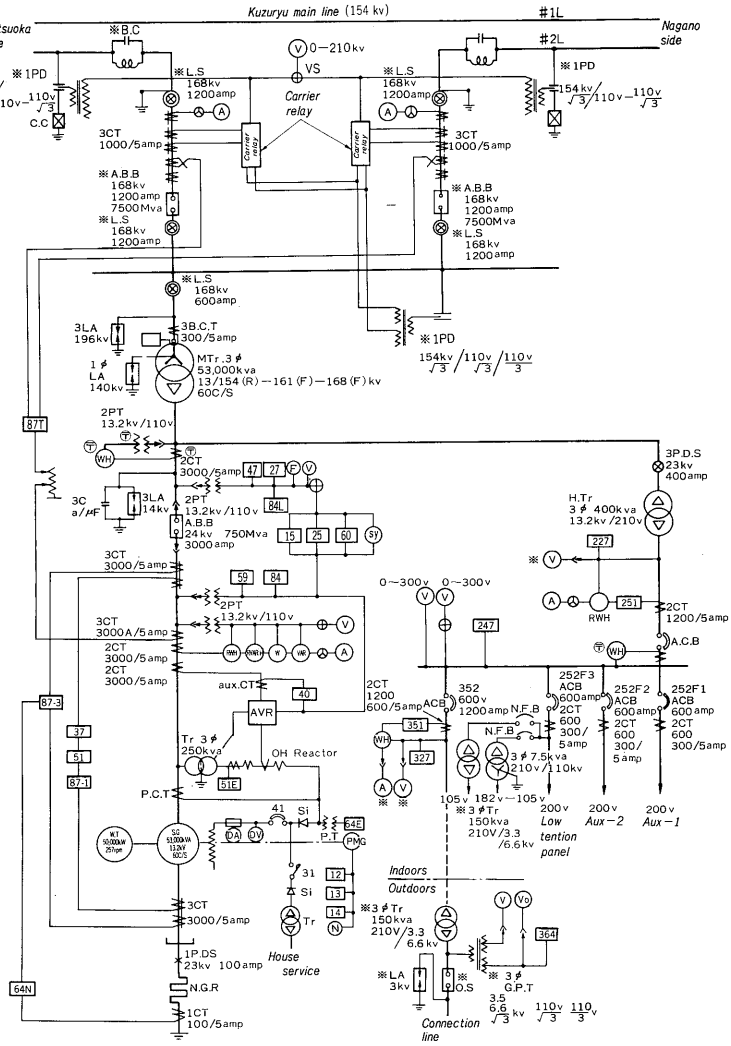

Fig. 22 Skeleton diagram

IV. OTHER DEVICES

1. Contactless Control Equipment and Contactless Protective Relays

In keeping with the progress made in all types of highly functional semiconductor elements, all kinds of control equipment and protective relays are now being changed to the contactless type. This contactless equipment has the following advantages when compared with previous contact-type devices.

(1) Operation hazards or erroneous operation due to long periods of use will not occur.
(2) There is no chance of misoperation due to contact wear or other reasons. Therefore maintenance is simple.
(3) Installation area is small

The scope of the adoption the contactless equipment in this power station is as follows:

1) Turbine control equipment

Turbine governor, control switch, limit switch, solenoid circuit, operation motor (77) circuit, etc.

2) Generator control equipment

Automatic voltage regulator, synchronous and parallel equipment, limit switch etc.

3) Protective relays

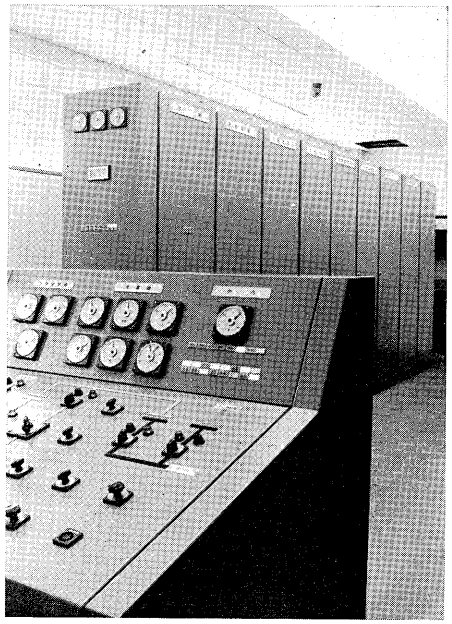

Fig. 23 Switchboad and control panel

87–1, 87–3, 51, 35, 59, 27, 64E, 40, 12, 13, 87T, etc.

4) Indication and alarm systems

Indication and alarm circuits required for main equipment operation, control and protection.

5) Tele-controlled equipment

As the equipment is changed to the contactless type, its reliability increases. However, since the operation of contactless equipment can not be checked merely by observation as with the former contact-type, problems of maintenance must be considered. Therefore, in order to insure easy maintenance and high reliability the following points were considered and have been incorporated in this equipment.

1) The protective relays are provided with checking circuits to indicate that the equipment is in order. In other words, by pushing a test button when required during operation of the equipment, the protective relays 86–1, 86–2 and 86–3 automatically perform a sequence of checks up to the turbine solenoid circuit and if any abnormality is present an alarm sounds. If operation is normal, an appropriate indication is given.

2) The start-stop control circuits carry out an automatic sequence of checks from the starting circuit to the synchronizing circuit breaker if a test button is pushed when required during stopping of the equipment. If any abnormality is present, an alarm sounds and if operation is normal, an appropriate indication is given.

3) Even if a fault should develop in the logic elements, the circuits are constructed so that mis-operation will never occur since there is an interlock system for other related elements.

4) When used in power equipment, the biggest problem is the possibility of abnormal voltages induced from power circuits but this is overcome by the use of arresters, surge killers, isolation transformers, etc.

V. CONCLUSION

This article contains an outline of the equipment supplied to Nishikadohara No. 3 Power Station.

Various kinds of site tests have been completed with satisfactory results as expected. Turbine efficiency tests by the current meter method and ultrasonic method both showed a high value of 93.4% and the curves from both methods were almost the same which confirmed the test results. The use of contactless equipment in this turbine was also of considerable significance and points toward future trends.